ORIGINAL PAPER

Synthesis of Isostearic Acid/Dimer Fatty Acid-Based Polyesteramide Polyol for the Development of Green Polyurethane Coatings

Pavan M. Paraskar[1] · Ravindra D. Kulkarni[1]

Abstract

Bio-based polyurethane (PU) coatings were prepared from novel branched isostearic acid (ISA) and long chains dimer fatty acid. Fatty amide was synthesized by the amidation of ISA with diethanolamine and the required hydroxyl functionality was developed via condensation polymerization with dimer fatty acid to produce polyesteramide polyol. The structure of the synthesized ISA based fatty amide (ISAFA) and polyesteramide polyol (ISAPEP) were identified using Fourier-transform infrared spectroscopy (FT-IR) and proton nuclear magnetic resonance (^{1}HNMR). The number average molecular weight of prepared polyesteramide polyol was assessed by gel permeation chromatography (GPC), while the rheological behavior was examined by the rheometer. Polyurethane metal coatings were developed from polyesteramide polyol, which crosslinks with hexamethylene diisocyanate (PU-H) and toluene diisocyanate (PU-T) and studied the influence of isocyanate structure on final PU coatings. A comparison in the crosslinks density of PU films was investigated by the gel content method. Differential scanning calorimetry (DSC) and thermo gravimetric analysis (TGA) were performed to evaluate the glass transition temperature (T_g) and thermal stability of the PU coatings. The surface roughness of prepared PU coatings was examined by Atomic force microscopy (AFM). The PU coated metal panels and films were examined for swelling resistance, hydrophobicity, mechanical, and coating properties. Results confirmed that bio-based long chain fatty acids provided hydrophobicity, flexibility and impact resistance to final PU coatings. It also noted that PU-T coating resulted in increasing thermal, mechanical, and coating properties compared to PU-H coating and this resulted from the structure of TDI, which contribute to higher crosslink density (i.e. presence of aromatic ring).

✉ Ravindra D. Kulkarni
    rd.kulkarni@ictmumbai.edu.in

    Pavan M. Paraskar
    pavan9970@gmail.com

1   Department of Oils, Oleochemicals and Surfactants
    Technology, Institute of Chemical Technology, Matunga (E),
    Mumbai 400019, India

Graphical Abstract
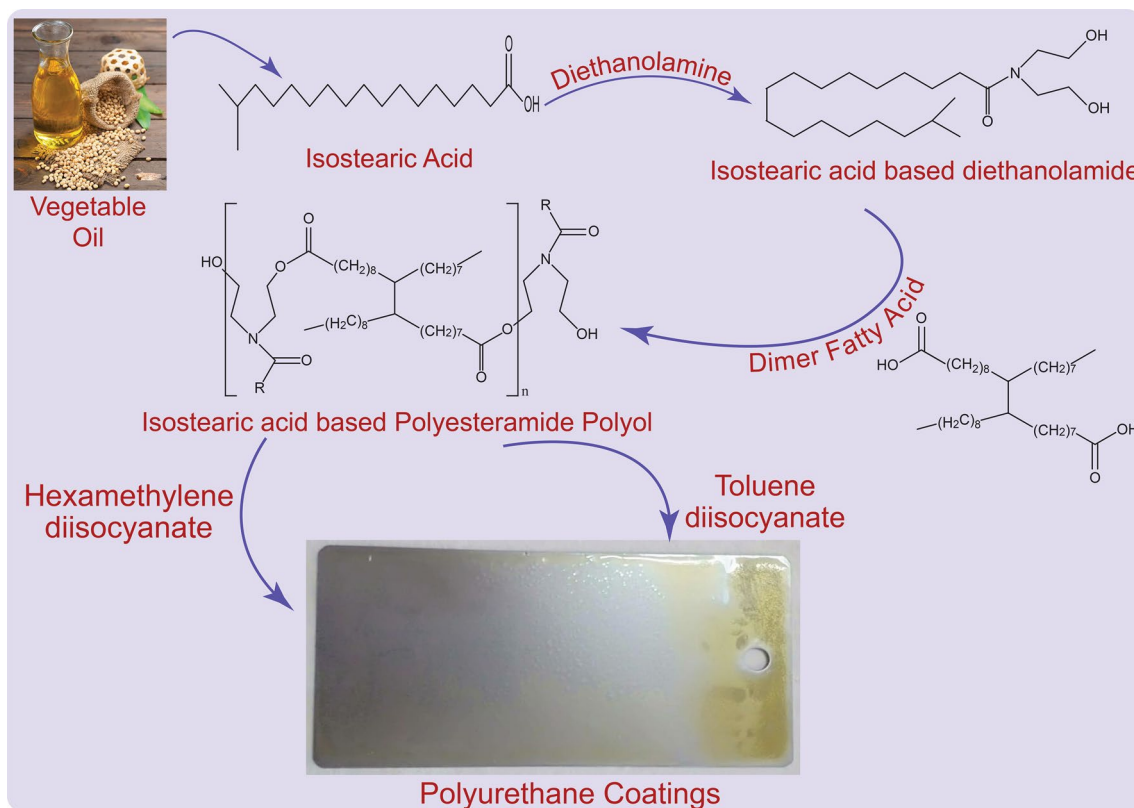
Introduction

The continuous depletion of fossil feedstock and alarming environmental pollution, bio-based materials have come to light for an environmentally friendly substitute to that, because of its high availability, sustainability, low carbon emission, and relatively low cost [1–4]. Amongst all the vegetable oils and their derivatives provide a viable alternative to petroleum-based feedstock and must be explored for further consideration [5–7]. Vegetable oil is essentially a triglyceride molecule that is arranged with different functional groups such as unsaturation [8], ester [9], and hydroxyl moiety [10]. One of the most widely used vegetable oil derivatives is a fatty acid which is obtained via hydrolysis of triglyceride [6]. Currently, the polymer industry has seen tremendous utilization of vegetable oil based polymers or intermediates such as polyamides [11], epoxy resin [12], polyester [13], polyesteramide [14], monoglycerides [15] and polyurethane [16]. The last decade has seen a boom in the research of the use of vegetable oils in the synthesis of polyurethane. Polyurethane is the most widely used polymer that has found applications in adhesives [17], elastomers

[18], thermosets [19], thermoplastics [20], coatings [21], sealants [22] and foams [23]. Recently, the usage of fatty acid shows encouraging performance as it provides control over the polyol structure. The utilization of fatty acids in polyol synthesis imparts lower viscosity and narrower molecular weight distribution over the mixture of fatty acids in the triglyceride structure [24, 25]. The various chemical modifications of vegetable oil and their derivative have been researched upon such as amidation-esterification [26], ozonolysis [27], epoxidation-ring opening [28], metathesis [24], and hydroformylation [7]. The most sought out synthesis route is the amidation-esterification route as it allows the integration of amide functionality in the synthesized polyol, which is beneficial as it improves various physical and chemical properties of the final polymer [29]. Dimer fatty acids (DA) are long chain dicarboxylic fatty acids obtained from C-18 unsaturated fatty acids (predominantly oleic acids) in the presence of clay [11]. Commercial manufacturing of dimer acids involves the utilization of oleic acid, linoleic acid and sometimes in combination with tall oil. The long hydrocarbon structure of dimer fatty acid provides hydrophobicity, flexibility and high stability to the final product

[30]. As they possess two reactive functional groups per molecule, they are considered to be excellent candidates for the synthesis of polyester polyols and polyurethane. Rajput et al. prepared polyurethane coatings for the wood substrate from dimer fatty acid via two-pack system [15]. During dimerization of fatty acids yields many by-products as well. A mixture of saturated branched-chain fatty acids is referred to as "Isostearic acid" which has a majority of branched C-18 fatty acids (68.3%) [31]. The unique branched structure of isostearic acid offers the derived copolymers with multitudinous desirable properties such as superior cold flow properties, low viscosity, excellent thermo-oxidative stability, and low melting point compared to its linear chain saturated and unsaturated analog [31–33]. These properties make isostearic acid an attractive raw material in the synthesis of polyurethane. To the best of our knowledge, no one has utilized the combination of branched isostearic acid and long chain dimer fatty acid to date in the synthesis of polyurethane. Therefore, in this study, we have synthesized isostearic acid based polyurethane in an attempt to prepared coating with numerous properties (hydrophobicity, impact resistance, thermo-oxidative stability) as well as offers sustainable alternatives for the replacement of fossil-based materials. Here we prepared polyesteramide polyol from bio based isostearic acid and dimer fatty acid and subsequently reacted with structurally different diisocyanates specifically hexamethylene diisocyanate (HDI) and toluene diisocyanate (TDI) to develop polyurethane coatings. The polyesteramide derived PU metal coatings were further examined for their

mechanical, physical, thermal, and surface roughness properties. Furthermore, the effect of the branched methyl group of isostearic acid on the properties of polyurethane was also investigated with a comparison to some existing studies.

Experimental Section

Materials

Isostearic acid (Prisorine 3501, Acid value = 185) and Dimer fatty acid (Pripol 1010, Acid value = 195) were obtained from Chroda Pvt. Ltd, Mumbai. The Isocyanate curing agents HDI and TDI were obtained from Covestro India Ltd. Mumbai. Dibutyltin dilaurate (DBTDL) was purchased from Sigma-Aldrich. Diethanolamine, xylene, diethyl ether, sodium methoxide, methyl ethyl ketone, and acetone were procured through Thomas Baker Pvt. Ltd, India. Mild steel (MS) panels of dimensions 6 × 3 cm were purchased from Komal Scientific. Pvt. Ltd. Mumbai. A 50-micron bar applicator was purchased from Khushboo Scientific, Pvt. Ltd. Mumbai India.

Synthesis of Fatty Amide

The reaction scheme for the synthesis of isostearic acid based fatty diethanolamide (ISAFA) is showed in Fig. 1. The reaction of diethanolamine with ISA taken in a 1:1 molar ratio in the presence of sodium methoxide as a catalyst.
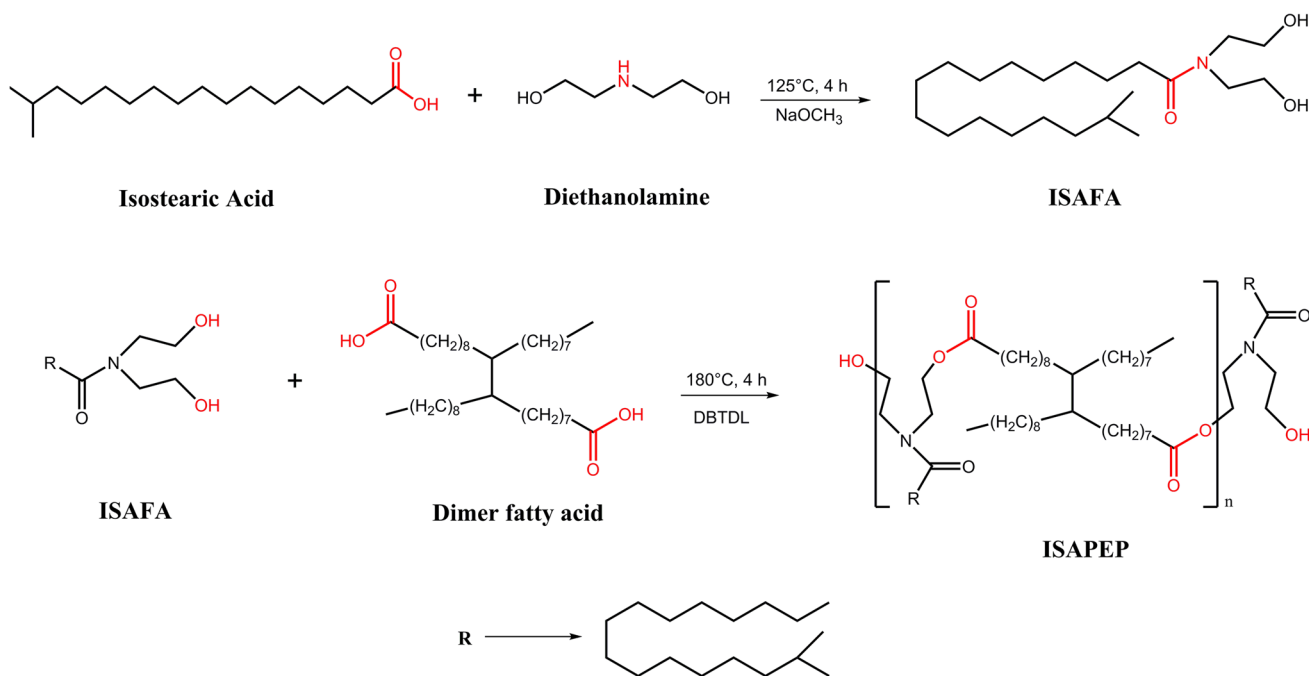

Fig. 1 Synthesis of isostearic acid based fatty amide (ISAFA) and polyesteramide polyol (ISAPEP)

Diethanolamine and sodium methoxide (0.5% by wt of fatty acid) was added to a 250-mL four-neck round bottom flask kept in an oil bath and equipped with an overhead stirrer, condenser, dropping funnel, and gas purger. The reaction mixture was stirred at 85 °C for 30 min in an N₂ atmosphere. ISA was added drop-wise into the reaction mixture up to 1 h and after complete addition, heating was continued for 3 h at 125 °C with continuous stirring. The progress of the reaction was checked by the regular determination of the acid value. Upon reaching an acid value below 5, the reaction was stopped by cooling the reaction mixture. The reaction mixture was given 15% brine solution washing followed bypasses through a bed of anhydrous sodium sulfate [29].

Synthesis of Polyesteramide Polyol

The reaction scheme for the synthesis of dimer fatty acid based polyesteramide polyol is given in Fig. 1. ISAPEP was prepared by the esterification reaction between dimer fatty acid (0.5 mol) and previously synthesized ISAFA (1 mol) in the presence of xylene as a reaction medium and DBTDL as a catalyst. All the components were charged to a four-necked round bottom flask equipped with nitrogen gas purger,

Dean-stark trap, overhead stirrer, and thermopocket. The reaction vessel was placed in an oil bath and the reaction was performed for 4 h at 185 °C with a nitrogen atmosphere. The water accumulated in the Dean-stark trap, as well as acid value analysis, were used to monitor the reaction progress. The reaction was stopped when the acid value attained below 5 mg of KOH/g of sample.

Preparation of Polyurethane Coatings (PU-H and PU-T)

Figures 2 and 3 shows reactions for the preparation of polyurethane coatings. Polyurethane coating denoted as PU-H was prepared by crosslinking ISAPEP with polymeric HDI in a two-pack system. ISAPEP and HDI were taken in 1:1.2 equivalent weight ratio of (OH: NCO) in the presence of DBTDL (0.05%) as a catalyst and xylene solvent in a beaker and mixed vigorously until desirable crosslinking action occurred. The extent of crosslinking was monitored by checking the Daniel flow of the resin. Before the application of PU coatings, the mild steel panels were scrubbed with sandpaper and wiped with acetone, and coatings were applied by using a 50 µm bar applicator. The coated panels
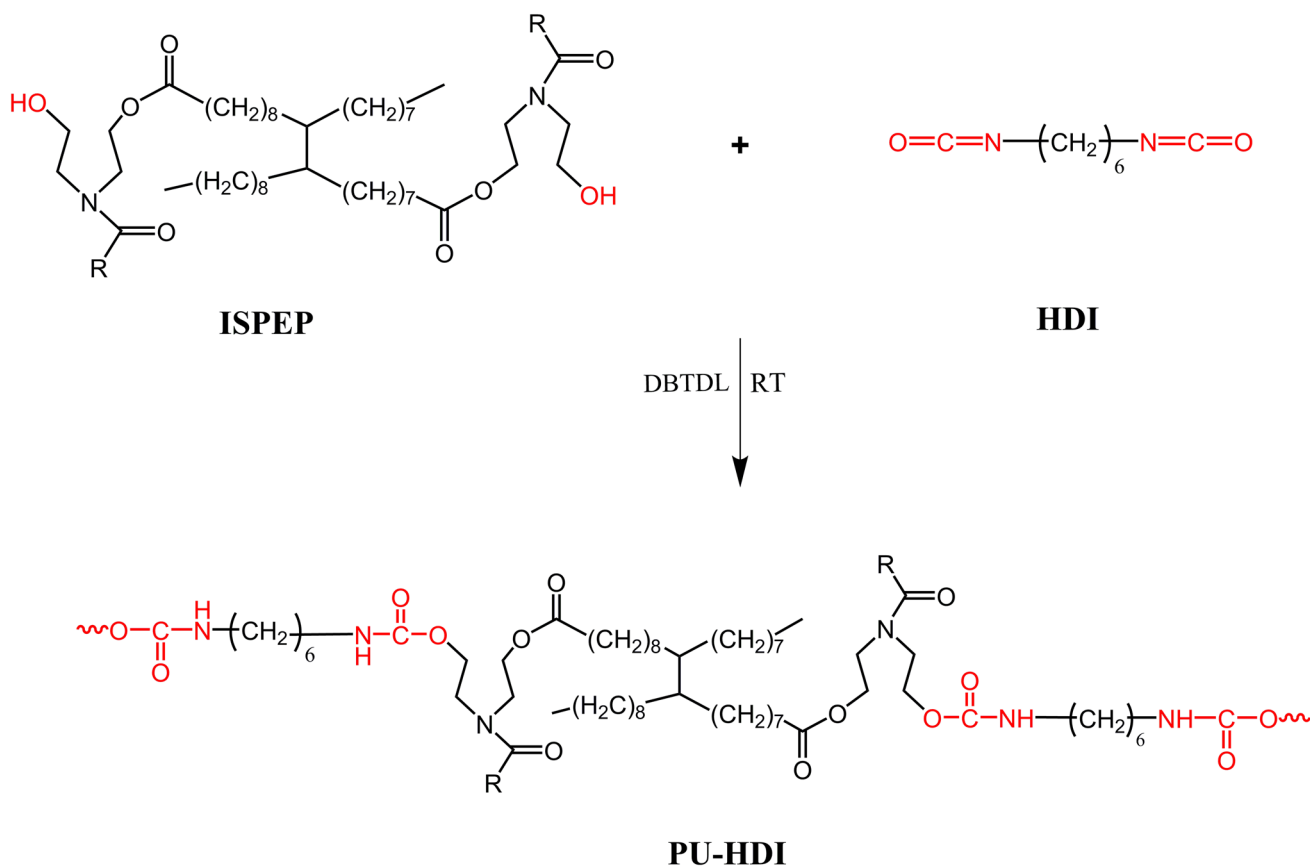

Fig. 2 Representative reaction scheme for preparation of polyurethane coating (PU-H)
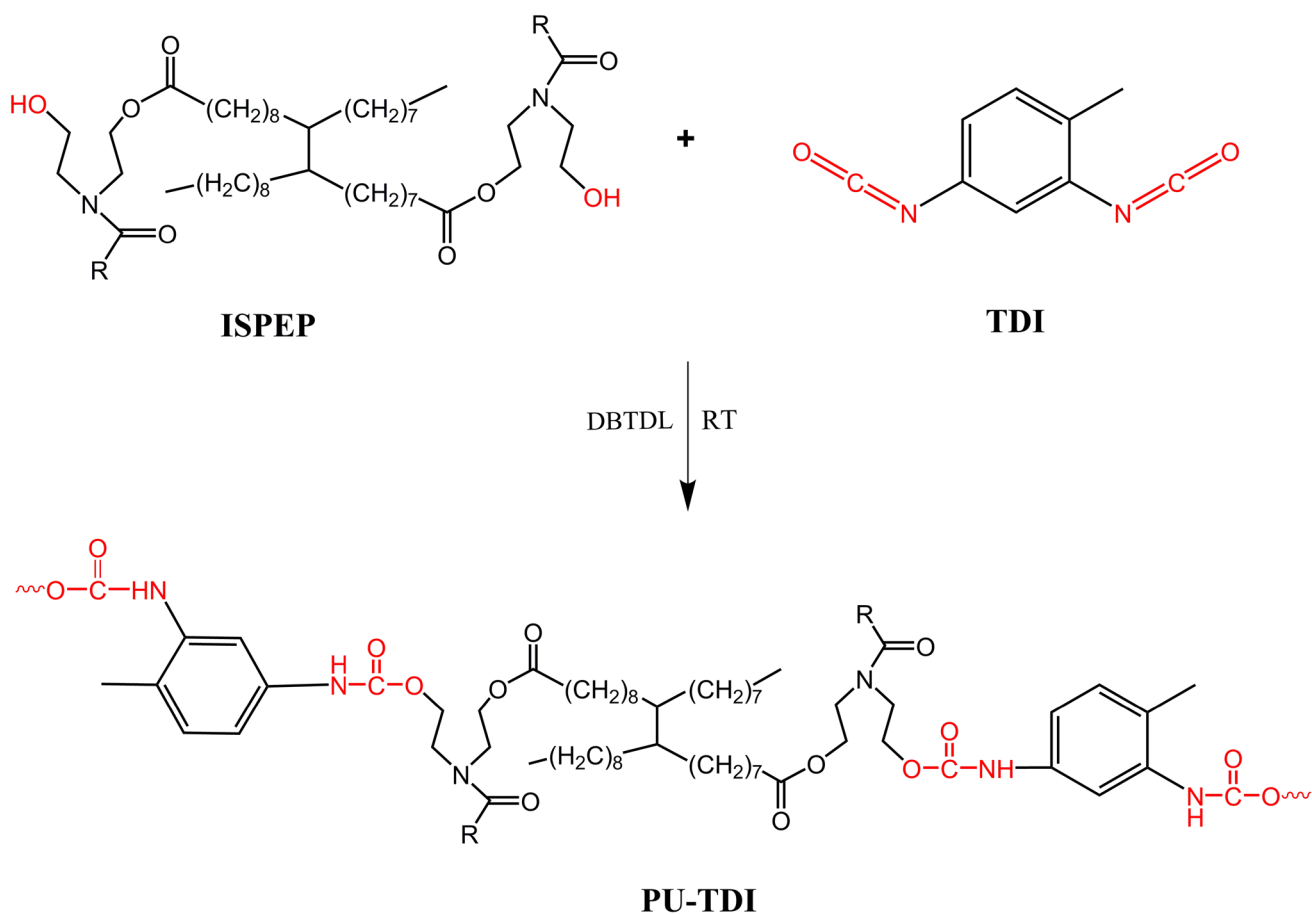
Fig. 3 Representative reaction scheme for preparation of polyurethane coating (PU-T)

were allowed to stand undisturbed for 8 h. Likewise, PU-T was prepared by reacting TDI with ISAPEP having a similar equivalent weight ratio.

Methods of Characterizations

End Group Analysis

ASTM and AOCS standards were referred to carry out end group analysis of synthesized products. The acid value (ASTM D 1980–87) of ISA and dimer fatty acid was analyzed through (Eq. 1). The acid value was utilized to determine the average molecular weight of ISA and dimer fatty acid (Eq. 2), which was used for stoichiometric calculations of amidation and esterification reactions.

$$\text{Acid Value} = \frac{56.11 \times A \times N}{B} \qquad (1)$$

where, A = Volume in ml of KOH required for the sample, N = Normality of the standard KOH solution, B = Weight in gm of a sample taken for the test

$$\text{Average molecular weight of ISA} = \frac{56100}{\text{Acid Value}} \qquad (2)$$

The % conversation of the amidation reaction and molecular weight of ISAFA was calculated using Eqs. 3 and 4.

% Conversion of amidation reaction

$$= \frac{\text{Acid value of initial reaction mixture} - \text{Acid value of ISAFA}}{\text{Acid value of initial reaction mixture}}$$

$$\times 100 \qquad (3)$$

$$\text{Molecular weight of ISAFA} = ((\text{M.W. of ISA} + 105.14) \\ \times (\% \text{ conversion}/100) - 18) \qquad (4)$$

The number of hydroxyl groups present in ISAPEP was evaluated using Hydroxyl value (AOCS Cd 13–60) (Eq. 5), which also used to calculate the equivalent weight of the polyol. The equivalent weight and reaction conversion of ISAPEP was calculated using Eqs. 6 and 7.

$$\text{Hydroxyl Value} = \frac{56.11 \times (A - B) \times N}{C} \qquad (5)$$

where, A = Volume of KOH solution (in mL) required for titration of the blank, B = Volume of KOH solution (in mL) required for titration of the sample, C = Weight of sample (in g), N = Normality of the KOH solution

$$\text{Equivalent weight of ISAPEP} = \frac{56100}{\text{Hydroxyl Value}} \quad (6)$$

% Conversion of polyesteramide polyol reaction

$$= \frac{\text{Actual amount of water formed}}{\text{Theoretical amount of water formed}} \times 100 \quad (7)$$

Instrumentation Techniques

To identify the functionality of the synthesized ISAFA and ISAPEP, FT-IR analyses were carried out on FT-IR 8400 (Shimadzu, Japan) with a range of 4000–400 cm^{-1} and resolution of 4 cm^{-1}. ^{1}H NMR spectra of ISAFA and ISAPEP were conducted by an Agilent Technologies 500-MHz instrument (recorded in CDCl$_3$ solvent and reporting the chemical shifts in ppm). The number average (Mn) molecular weight, weight average (Mw) molecular weight and polydispersity index (PDI) of polyesteramide polyol was analyzed through gel permeation chromatography (Agilent GPC-Addon).The sample was dissolved in tetrahydrofuran to give an accurate concentration at 5–6 mg ml^{-1}. For GPC calibration, a concentration of 2 mg ml^{-1} of each of the polystyrene standards was used. Rheological properties of resin were investigated by Rheometer 9MCR 101, (Anton Paar, Austria) including parallel plat assembly. During the rheological analysis, the rheometer cone was maintained at a distance of 0.5 mm from its plate (diameter–25 mm. The glass transition temperature (T$_g$) of cured PU films was evaluated using Hitachi 7020 differential scanning calorimetry (DSC) with a heating range of 20 °C to 300 °C and a rate of 10 °C min^{-1}, in inert nitrogen condition. The thermo gravimetric analysis (TGA) of cured PU coatings were conducted on TA- Discovery 55, (USA) with a heating range of 20 °C to 600 °C at a rate of 10 °C per minute, and nitrogen gas stream. Contact angle measurement (CA) (sessile drop method), was conducted on a DMO 601 Kyowa Interface Science (Japan) dynamic contact angle meter, to evaluate the hydrophilic-hydrophobic properties of cured PU coating surface. The surface properties of PU coatings were recorded on Asylum Research oxford (model No.: MFP-3D), Atomic force microscope (AFM). Roughness was calculated over a sample area of 100 µm^2.

Cured Coatings Characterizations

Mechanical properties of the PU films were tested on Universal Testing Machine UTM (2302 R & D Equipment, Mumbai) using 50 N load cell with a crosshead speed of 5 mm/min. The film sample was cut in measurements of 12 cm × 1 cm with a film thickness of 150–200 µ. The cured PU-H and PU-T samples were subjected to several mechanical and surface tests for evaluation. The gloss of cured coating was measured, at an angle of 60°, using a calibrated digital gloss meter (Khushboo Scientific, Pvt. Ltd. Mumbai India). The impact resistance (ASTM D-2794) of the coating was tested by dropping a 2 kg. load from an elevation of 80 cm on to the coated side of the panel. The thickness of the cured film was measured with a dry film thickness gauge (calibrated). Referring to ASTM D-522, a conical mandrel tester (Komal Scientific, Pvt. Ltd. Mumbai) was used to assess the coating flexibility by bending the panel at different angles in the range of 45°–180°. Pencil hardness (ASTM D-3363) of cured coatings was evaluated using a pencil hardness tester (Raj Scientific, Mumbai India). The adhesion property of coating was assessed using a cross-cut test (ASTM D-3359) which involves applying adhesive tape over a lattice mark (till the metal surface was exposed) of 1 cm^2 on the coating. After ripping off the tape, standards were referred to evaluate the extent of adhesion failure. Scratch hardness (IS-104), which involves allowing a needle to move over the coating with a gradually increasing amount of weight acting on it until the film breaks, was also conducted on the panel. The tests were conducted in triplets to obtain more precise readings. Ethanol, water, and toluene were used to examine the swelling properties (S) (Eq. 8) of cured PU coatings. Weighed samples were placed in solvents for 50 h at ambient temperatures, followed by drying and weighing.

$$\% \, S = \frac{W_2 - W_1}{W_2} \times 100 \quad (8)$$

where, W$_1$ = weight of the cured sample before immersion in the solvent, W$_2$ = weight of the sample after immersion in the solvent.

Gel content (ASTM D 2765-01) of cured PU films helped to examine their crosslink density. Before testing, the 1 g samples were vacuum dried at 40 °C for 2 days. The empty filter paper pouch and the pouch with the dried film placed in it were both weighed with weights W1 and W2 respectively. The pouch was stapled sealed and was again weighed (W3). For a period of 24 h, the film carrying sealed pouch was placed in a xylene refluxing Soxhlet apparatus. The pouch was dried at 150 °C in a vacuum oven and weighed to a constant weight (W4). The test was

conducted in triplets for precise readings. The gel content (Gc) for the cured films was calculated using the Eq. (9).

$$G_c(\%) = 100 - \left(\frac{W_3 - W_4}{W_2 - W_1} \times 100 \right) \quad (9)$$

Result and Discussion

### Physicochemical Properties of Fatty Diethanolamide and Polyesteramide Polyol

End group analysis of fatty acid based fatty diethanolamide is depicted in Table 1. The ISAFA was prepared by the reaction of ISA with diethanolamine. The advancement and conversion of the reaction were calculated by the decreases in acid value. Initially, the acid value of the reaction mixture

Table 1 Physico-chemical properties of ISAFA and ISAPEP

Physico-chemical properties/code of samples	ISAFA	ISAPEP
Acid value (mg of KOH/g of sample)	3.6 ± 0.4	1.9 ± 0.5
Hydroxyl value (mg of KOH/g of sample)	141 ± 2.1	102 ± 2.6
% Conversion of reaction	98.05%	95.65%
Average molecular weight (g/mol)	382.5 ± 2.7	550 ± 3.1

is 185 which is attributed to the acid groups present in ISA. After the completion of the reaction, the acid value (3.6 mg. of KOH/g) was dropped down significantly as shown in Fig. 4, which signifies the consumption ISA acid in the desired reaction to yield fatty amides. The % conversion (Eq. 3) of the reaction was determined by a decrease in acid value and was achieved to be 98.05%. The average molecular weight of ISAFA (Eq. 4) was determined from % conversion of amidation reaction and it was to be 382.5 g/mol. The Physicochemical properties of polyesteramide polyol are described in Table 1. The ISAPEP prepared via esterification reaction between dimer fatty acid and previously prepared ISAFA. The extent of reaction was controlled by comparing the actual and expected water as a by-product, as well as calculating the acid value of the reaction mixture periodically. The progress of the esterification reaction to yield the desired hydroxyl groups can be seen by the continuous drop in the acid value as shown in Fig. 4. The yield of reaction (Eq. 7) was determined to be 95.65%. The equivalent weight (Eq. 6) of the ISAPEP was calculated by utilizing the hydroxyl value (102 mg of KOH/g) and was found to be 550 g/mol.

Fig. 4 Graph of acid residue content of ISAFA and ISAPEP during reaction versus time
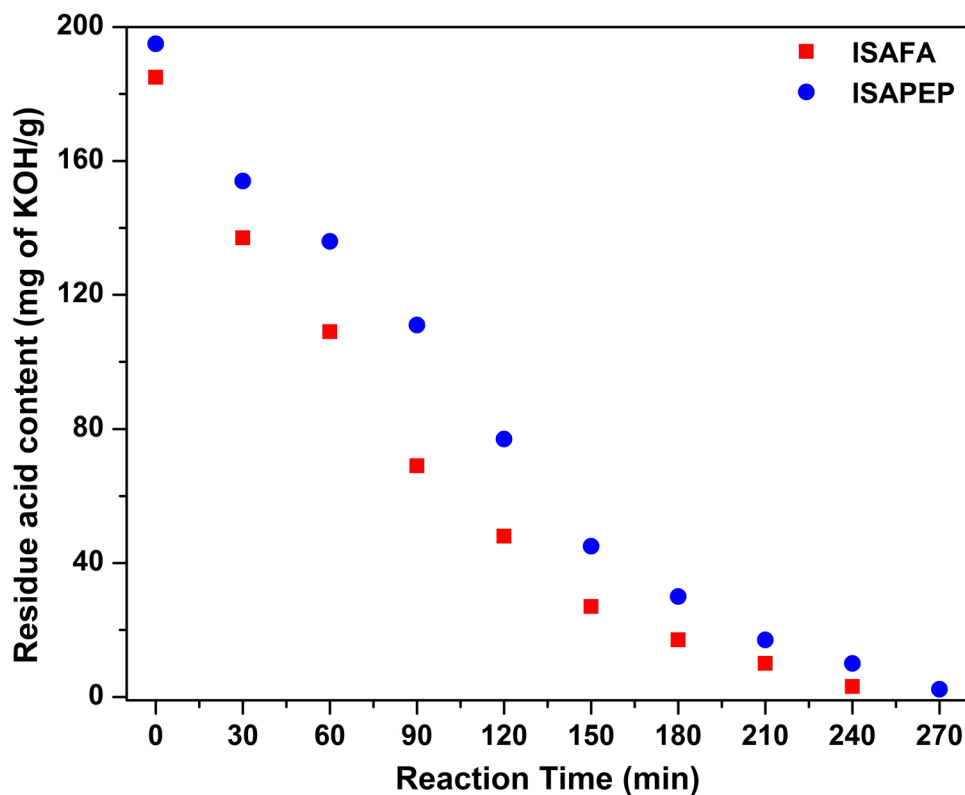
Rheology Behavior of Fatty Amide and Polyesteramide Polyol

As we know the viscosity of resin impacts the nature of the applied coatings [34]. It may influence the thickness of the coating, spreading ability, film formation, adhesion, and levelling. The rheological behavior of ISA, ISAFA and ISAPEP at various shear rates is analyzed and results are presents in Fig. 5. Upon the reaction of ISA with diethanolamine, there was an improvement in viscosity because of rising in the molecular weight of polymer structure (ISAFA). Furthermore, ISAPEP exhibited higher viscosity than ISA and ISAFA, which was mainly because of the contribution of amine long chain fatty acid from dimer acid in the molecular structure of resulting polyesteramide polyol. The higher molecular weight of polyol showed non-Newtonian behavior.

Molecular Weight Distribution of ISAPEP

The GPC curve and the corresponding molecular weight distribution values of the ISAPEP is represented in Fig. 6. The results exhibited that the number average molecular weight (Mn) and weight average molecular weight (Mw) of ISAPEP were 379 and 840 respectively. The polydispersity index (PDI) of the ISAPEP was found 2.21, which shows that prepared polyol has broad molecular weight distribution.

FTIR Analysis

Figure 7 shows the FTIR spectrum of ISAFA and ISAPEP. The broad absorption peak for –OH group stretching existing in ISAFA was noticed at the range of 3223–3496 cm^{-1}. The characteristic peak at 1630 cm^{-1} and 1459 cm^{-1} are attributed to the stretching frequency of amide carbonyl (C=O) and an amide linkage (C–N) [26]. The absorption peak at 1738 cm^{-1} corresponding to the stretching frequency of the ester carbonyl (–C=O). The characteristics peak at range of 2861–2936 cm^{-1} represent CH_2 symmetric and asymmetric stretching of long chain fatty acid. The appearance of an amide absorption peak and the disappearance of amine functionality confirmed the synthesis of ISAFA. The FT-IR spectra of ISAPEP showed the broad absorption peak for OH stretching at a range of 3329–3500 cm^{-1}. The characteristics peak at 2853 and 2921 cm^{-1} is attributed to CH_2 symmetric and asymmetric stretching present in ISAPEP. The appearance of characteristic peaks at 1739 cm^{-1}, 1655 and 1460 cm^{-1} indicated stretching frequency of ester carbonyl (–COOR), amide carbonyl (-CON-) and amide linkages (C–N) respectively. Additionally, in the ISAPEP FT-IR spectra, peaks at 1166 cm^{-1} corresponded to the stretching vibration of -C−O-, however, the absence of this absorption peak in the ISAFA FT-IR spectra proves successful formation of ester linkages.

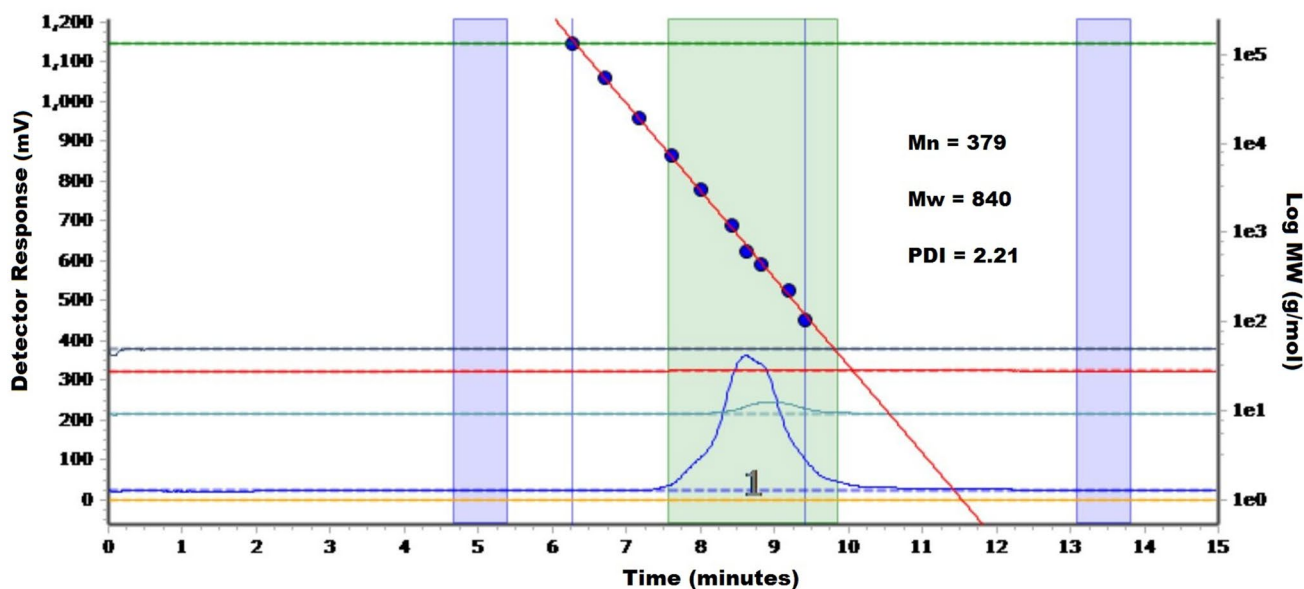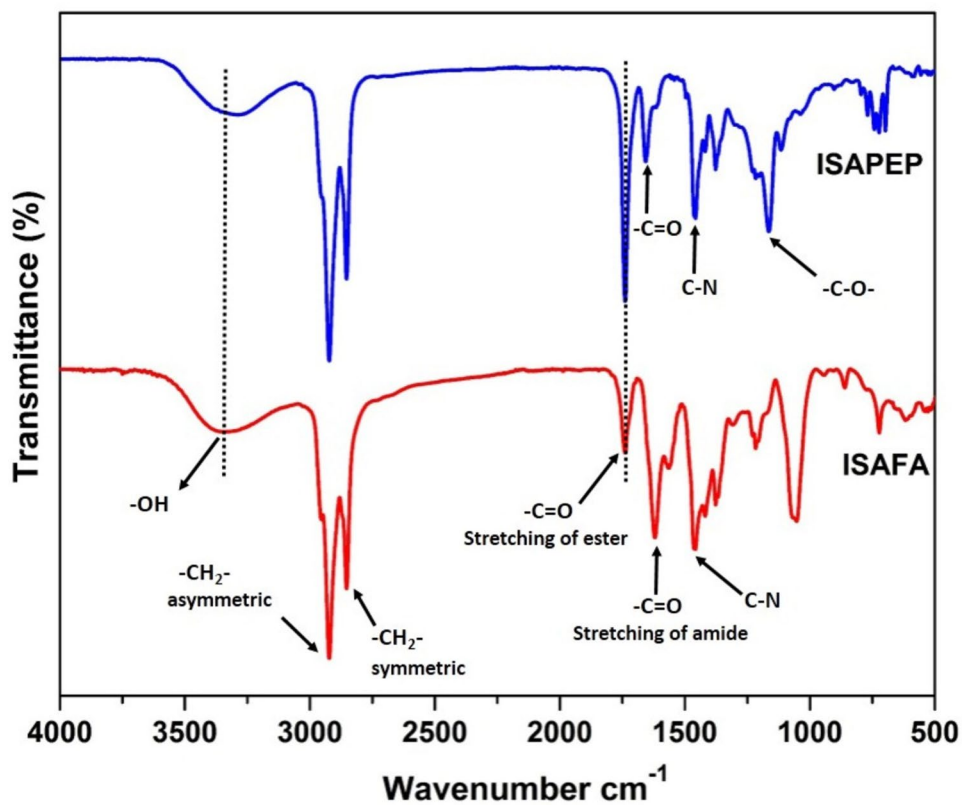**Fig. 5** Rheological behavior of ISA, ISAFA, ISAPEP
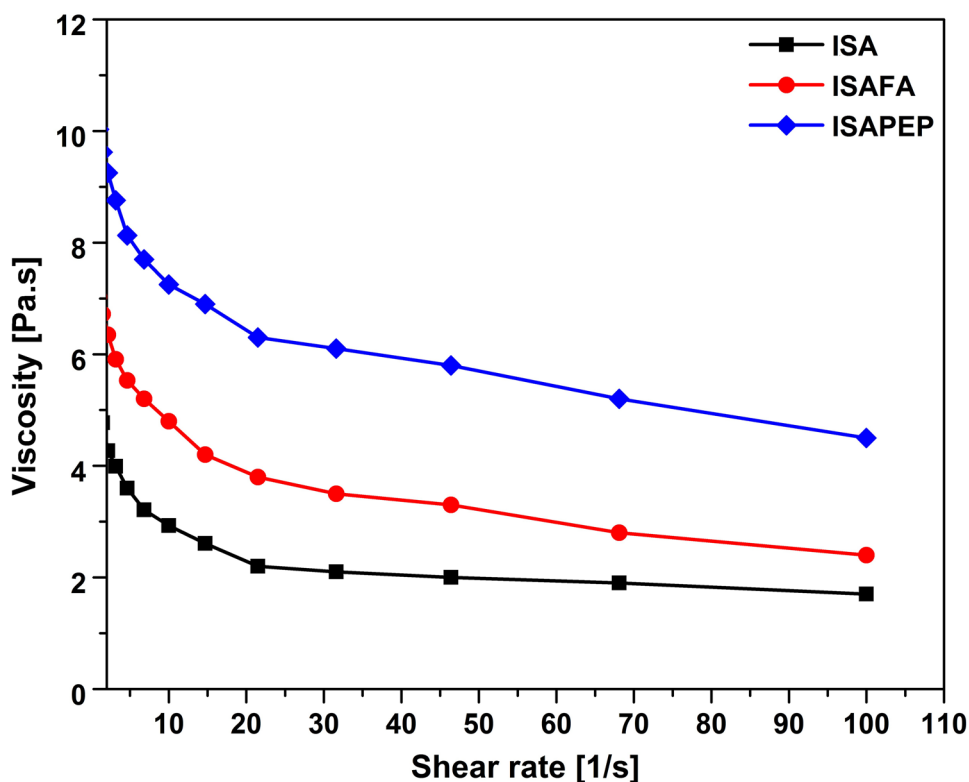
Fig. 6 Gel permeation chromatograph of ISAPEP

Fig. 7 FT-IR spectra of ISAFA and ISAPEP

¹H-NMR Analysis

The molecular structure of ISAFA and ISAPEP was studied by ¹H NMR. Figure 8 shows the spectrum ISAFA, the peak at δ = 0.83 ppm (1) attributes to terminal methyl groups, while the peak obtained at δ = 1.10–1.33 ppm (3) represent internal –CH₂– groups present in the isostearic fatty acid chain. The peak appeared at δ = 1.59 ppm (2) attributed to the –CH– group proton, which is existing between the internal –CH₂– groups and terminal methyl groups. The signal

Fig. 8 ^{1}H NMR analysis of isostearic acid based fatty amide (ISAFA)
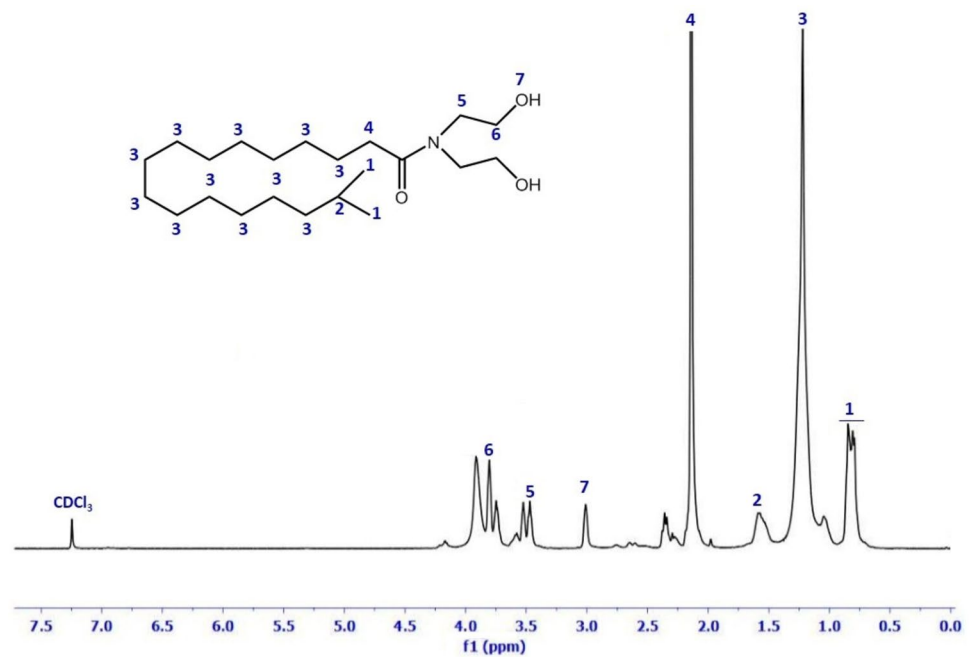
obtained at δ = 2.22 ppm (4) corresponds to the proton of the –CH$_2$- group linked to carbonyl functionality. The peak obtained at δ = 3.43–3.51 ppm (5) corresponds to the proton of –CH$_2$- group linked to amide linkage, while the proton of –CH$_2$– group attached to the terminal hydroxyl group caught at δ = 3.70–3.73 ppm (6) [15]. The peak detected at δ = 3.00 ppm (7) belongs to the primary –OH from ISAFA. Thus the ^{1}H-NMR spectra were used to confirm the molecular structure of fatty amide. The ^{1}H-NMR spectra for ISAPEP are shown in Fig. 9. The proton of the terminal
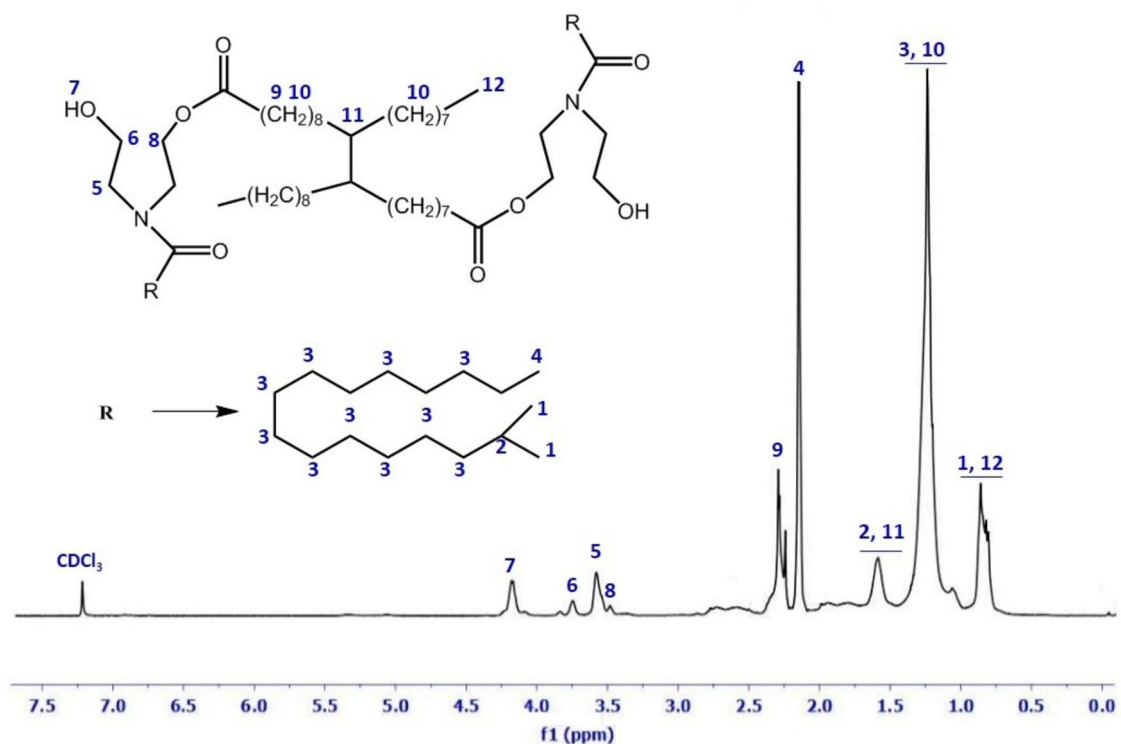

Fig. 9 ^{1}H NMR analysis of isostearic acid based polyesteramide polyol (ISAPEP)

methyl groups detected at δ = 0.85 ppm (1,12), while the proton of the internal –CH$_2$– groups present in the long fatty acid chain observed at δ = 1.10–1.31 ppm (3,10). The peak obtained at δ = 1.59 ppm (2, 11) corresponds to the methine group proton, which is existing between the terminal methyl groups and internal –CH$_2$– groups. The peak appeared at δ = 2.28 (4) and δ = 2.33 ppm (9) were characteristics for –CH$_2$– attached to carbonyl amide functionality and –CH$_2$– attached to ester functionality respectively [30]. The peak appeared at δ = 3.6 ppm (5) was attributed to –CH$_2$– group linked to amide nitrogen and the peak obtained at δ = 3.75 ppm (6) attributed to the proton of –CH$_2$– besides to –OH group. The peak appeared at δ = 3.41 ppm (8) attributed to the –CH$_2$– group proton, which is present between the ester functionality and –CH$_2$– group adjacent to amide linkage. The sharp peak observed at δ = 4.12 ppm (7) associated with –OH group from ISAPEP. Therefore the ^{1}H-NMR spectra were used to verify the molecular structure of isostearic acid based polyesteramide polyol.

Gel Content

Gel content is an important factor, which directly impacts the properties of cured PU coatings. There is a direct relationship between gel content and extent of crosslink density as higher the crosslink density, lesser will be the insoluble polymers present in the cured film and lesser will be the gel content. The results for gel content are presented in Table 2. The result exhibits that the PU-H cured coating had lower gel content compared to the coating cured with PU-T, which indicates that the higher reactivity of isocyanate toward the OH and aromatic structure of TDI promotes high crosslinking and thus increased crosslinking density.

DSC Analysis of Cured PU Coatings

Generally, glass transition temperature (T$_g$) of the polymer mainly depends on intermolecular interaction, chain segment mobility, and crosslink density of a polymer [16]. The influence in T$_g$ is directly co-relate with crosslink density which depends on the functionality of the resin and hardener. In that case, TDI with the aromatic ring can impact the T$_g$ together with additional factors like crosslink density and the long fatty acid chain from the polyesteramide polyol. The T$_g$ values of cured PU coatings were recorded based

on endothermic peaks of their second heating DSC curves. Figure 10 shows glass transition temperature (T$_g$) of PU-H and PUT coatings as 53.08 and 64.18 °C respectively. The PU-T based coating showed higher T$_g$ values compared to PU-H coating, which can be assigned to the higher crosslink density of the coating. The higher T$_g$ values of PU-T coating may be attributed to a higher extent of crosslinking of coatings due to its higher reactivity and rigid structure of TDI, while PU-H coating show lower T$_g$ values because of low reactivity and aliphatic structure of HDI. Moreover, the T$_g$ values also affected by the structure of the polyol in which the branched methyl group may influence the chain mobility. The enhanced crosslink density decreases the chain segment mobility, in this manner extra energy required to molecular segments order to achieve smooth region [2].

Thermo Gravimetric Analysis of Cured PU Coatings

Thermo gravimetric analysis (TGA) is a widely used method that examined the thermal stability of materials and assessing the fractions of volatile components by monitoring the weight change [35]. The thermal stability of PU coatings mostly depended on the structure of isocyanate (hard segment) and polyol (soft segment). The thermo-oxidative degradation process of cured PU coatings with different isocyanate is demonstrated in Fig. 11 and related data for 5% and 30% weight loss temperature (T5, T30) and char residue at 600 °C are depicted in Table 3. TGA curves for both PU-H and PU-T samples exhibited two steps of degradation. Initially, 5% of weight loss for both PU-H and PU-T coatings at 210–219 °C correspond to entrapped air and volatile matter. The first degradation step of the PU-H appeared at 263–352 °C and degradation resulted in a 50% weight loss. The second degradation step happened at 365–490 °C with corresponding weight losses in the range of 43% and this step exhibits slow-moving degradation. The first degradation step of the PU-T coating was occurred at 272 °C and finished at 388 °C with degradation resulted in a 30% weight loss. In the second step of degradation, the onset temperature for PU-T coating was between 390 and 498 °C with 63% weight loss. The first step degradation is attributed to the decomposition of urethane linkages (hard segment), which results in the formation of isocyanate, primary or secondary amine and alcohols [36]. The second step degradation is assigned

Table 2 Mechanical, swelling property and gel content of cured PU coatings

Sample code	Tensile strength (Mpa)	Elongation at break (%)	Young modulus (Mpa)	Swelling (%)			Gel content (%)
				Water	Ethanol	Toluene	
PU-H	10.7 ± 1.7	6.34 ± 0.8	391.39 ± 3.4	4.2 ± 0.6	5.8 ± 0.5	7.2 ± 1.5	94.53 ± 0.75
PU-T	15.5 ± 0.6	4.27 ± 0.3	452.36 ± 3.3	3.3 ± 0.9	3.8 ± 0.2	5.3 ± 1.7	97.89 ± 0.68

Fig. 10 DSC analysis of cured PU coatings
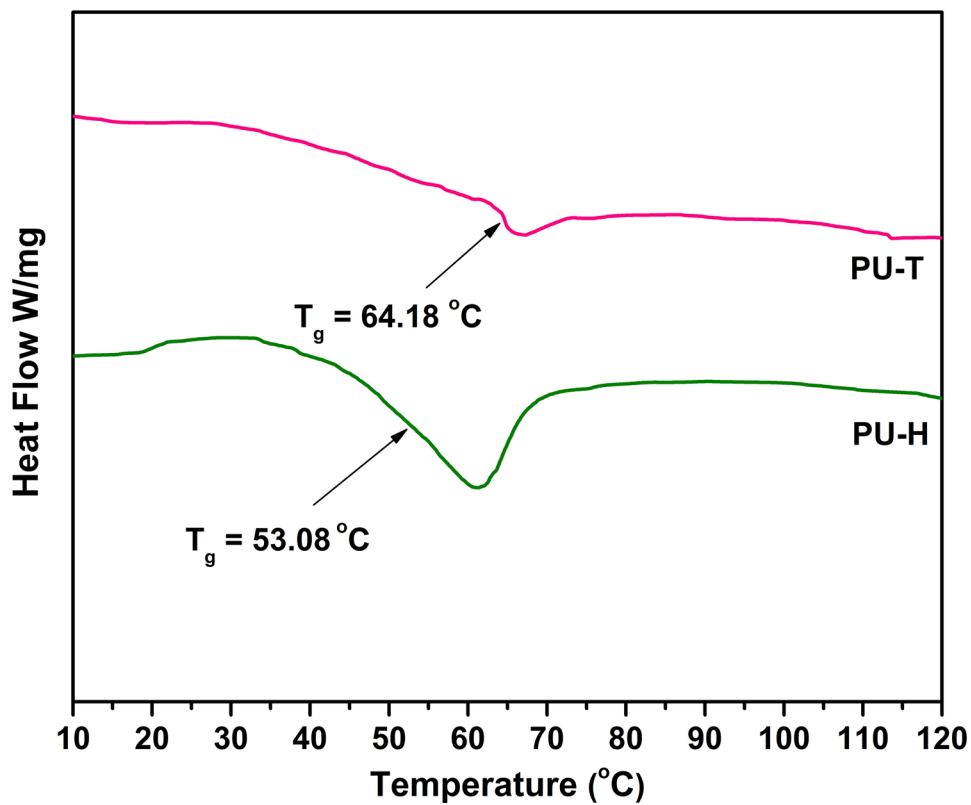

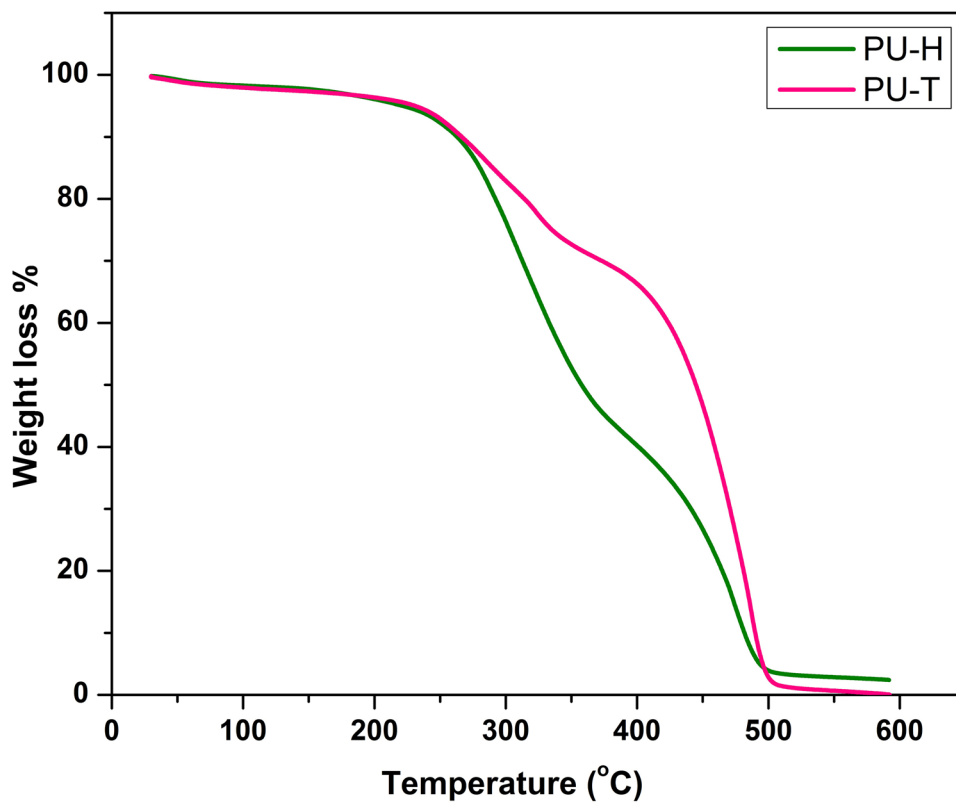**Fig. 11** TGA thermogram of cured PU coatings

Table 3 Thermal analysis of cured PU coatings

Sample code	T5 (°C)	T30 (°C)	T50 (°C)	Charred residue at 600 (°C) (%)	Ts (°C)
PU-H	210.21	312.16	352.31	1.35	132.97
PU-T	219.24	388.31	446.37	1.26	157.25

Table 4 Surface and physico-mechanical properties of PU coatings

Properties	PU-H	PU-T
Pot life (h)	3	2.5
Surface drying (min)	30	25
Tack free drying (h)	2.5	2
Hard drying (h)	8	7.5
Gloss (°)	96 ± 3	108 ± 3
Thickness (μ)	47 ± 1	47 ± 1.3
Adhesion (Cross-hatch) (%)	100	100
Flexibility 1/8″ bending mandrel	Pass	Pass
Scratch hardness (kg)	2.1 ± 0.2	2.4 ± 0.2
Impact resistance lb. in	141 ± 1.3	148 ± 1.5
Pencil hardness	3H	4H
Contact angle (°)	108 ± 2	115 ± 2
Root mean roughness (nm)	9.24	15.37

to the thermal decomposition of ester moieties, amide linkages, and hydrocarbons chain present in PU coating (soft segment) [30, 37]. The thermal stability of PU coatings was also evaluated using statistic heat resistance index temperature (Ts) which was calculated from Eq. (10).

$$Ts = 0.49[Td5 + 0.6(Td30 - Td5)] \tag{10}$$

where, Td5-temperature of 5% weight loss, Td30- temperature of 30% weight loss.

It is noticeable from Table 3 and Fig. 11 that the PU-T coating showed higher thermal stability compared to PU-H coating, which can be assigned to the higher crosslink density of the coating. The higher crosslinking density arises from higher reactivity of TDI, because of the aromatic ring present in it. Additionally, it also can be assumed that branched methyl group of isostearic acid restricts the chain segment mobility of polymer and enhanced thermal stability [38]**.** The present study exhibited better thermal stability compared to our earlier work [26].

Evaluation of Surface and Physico-Mechanical Properties

The surface properties of PU coatings presented in Table 4. The pot life of PU-T and PU-H coatings obtained at ambient condition was found to be 3 h. The coatings applied on the metal panel took 25 to 30 min for drying while tack free drying required 2 to 2.5 h. The surface drying and hard drying time were observed to be fastest for PU-T because of the higher reactivity and aromatic ring present in TDI, which promote faster curing. Hard drying of PU-T and PU-H was achieved over 7.5 and 8 h respectively. The thickness of PU-T and PU-H was found to be 47μ. Gloss was found to be 108° for PU-T and 96° for PU-H coatings respectively. The higher gloss of the PU-T system could be assigned to the existence of an aromatic ring in the TDI hardener, which leads to a higher extent of crosslinking. The coating also maintained excellent dimensional stability and smooth surface that enhanced the gloss of PU-T coating [39]. The cured PU coatings panels are bent to 180° following the conical mandrel tester. After bending, if the coating is neither removed nor cracked then it is said to be passed. Polyesteramide polyol will fully use the saturated fatty acids likewise offer longer structure chains, suitable in flexible applications. Both the coatings passed the flexibility test due to the combination of a long aliphatic chain of dimer acid and non-crystallinity in the polyol structure that contribute to better flexibility of the PU coatings. Both PU coatings passed the impact test as none of them shows any indication of breaking upon impact test. This superior impact resistance is attributed to the fatty acid chain contributed by isostearic acid as well as the long fatty acids chains of dimer fatty in the soft segments of polyol and hardness offered from high crosslink density of PU structure. Compared to vegetable oil based coating in the earlier study, a coating with the highest impact resistance of 70.86 lb.in [16] and in present research the highest impact resistance of 148 lb.in which shows that fatty acid based coating is more flexible and can be applied for developing high-performance coatings. PU-T coating indicated scratch after the application of 4H pencil due to more cross-link density of coating arising from the rigid structure of TDI while the PU-H coating showed scratch upon the application of 3H pencil due to more flexible structure of HDI. It could be attributed to the uniform, optimum cross-linked, and well-adhered structure of the PU coating [40]. The scratch hardness for both coatings was found to be 2.4 kg for PU-T and 2.1 kg for PU-H respectively. The higher scratch hardness of PU-T coating could be attributed to the aromatic ring in the TDI hardener, which leads to a higher extent of crosslinking and responsible for the surface hardness of the coatings. Additionally, the presence of polar groups and hydrogen

bonding in PU backbone increases the surface hardness and provided an excellent scratch hardness and pencil hardness to the prepared coatings. The present study of fatty acid based PU coating shows high values for scratch hardness and pencil hardness compared to the reported fatty acid based PU coating [15]. Both PU coatings show 100% adhesion to the metal substrates as measured by the cross-cut adhesion test. The N–H group from urethanes linkage created a hydrogen bond with the metal substrate and improve its adhesion property [41]. Additionally, the morphology of the isostearic fatty acid structure inside the polyesteramide polyol makes a substantial improvement in the adhesion. Considering the above-mentioned physicomechanical characteristics, the final PU coating properties are affected by the rigid structure of TDI and flexible structure of HDI, as well as, presence of long aliphatic chains in isostearic acid and dimer fatty acid.

Mechanical Properties of PU Coatings

Generally, mechanical properties of a polymer rely on various parameters like the existence of polar groups within the polymeric chains, hydrogen bonding, presence of inter and intra-molecular interactions, molecular weight, and compositions of the reactants. The cross-link density would also influence the tensile properties and elongation of the PU coating [42]. The hard segment from PU creates ordered domains due to hydrogen bonding and provide high strength and rigidity to the material, while the soft segments from PU provides elastic properties to the material. The mechanical properties of PU coatings were studied by tensile strength, young modulus and elongation at break and presented in Table 2. As can see (Table 2) PU-T coating exhibited higher tensile strength (15.5 Mpa) and young modulus (452.36 Mpa) compared to PU-H coating's tensile strength (10.7 Mpa) and young modulus (391.39 Mpa). Increasing the crosslinking density of polymer backbone reducing the mobility of chain segments and increases of tensile strength and young modulus of PU-T coatings [43]. This is because of the high reactivity and aromatic structure of TDI (hard segment), which imparted more stiffness and rigidity to the final cured PU-T coatings. Moreover, PU-H coating exhibited higher elongation at break (6.34%) compared to PU-T (4.27%). This is because of the aliphatic structure of HDI as well as the presence of long fatty acids chains in polyol (soft segment), which provides extra flexibility to PU-H coating hence improved elongation at break [44].

Swelling Properties of PU Coatings

The swelling test was performed to examine the resistance of the PU coatings towards the water and organic solvents (toluene and ethanol) and the finding are presented in Table 2. Both PU coatings showed superior resistance to water than to organic solvents because the hydrocarbon character leads the fatty acid and derived polymers extremely hydrophobic. Hence, the hydrophobic nature of fatty acid chains presence in polyol seems to play an important role than the presence of ester bonds. Moreover, it is notable that the steric effect of methyl group of the isostearic acid helped to improve the swelling properties of the PU coating [45]. Besides, higher reactivity and aromatic structure of PU-T favored diminishing the swelling of which was usually attributed to the improvement of crosslinking. Additionally, it was indicated that PU-H coating showed inferior swelling resistance compared to PU-T coating due to the aliphatic structure of HDI, which lowers the crosslink density of the coating.

Hydrophobic Properties of PU Coatings

Water contact angle (WCA) is used to examine the hydrophobic and hydrophilic character of the cured PU coatings surface. If the contact angle is more than 150°, the surface is said to be ultra-hydrophobic, contact angle below 90° it is considered as hydrophilic and contact angle 90°–150° it is considered as hydrophobic [29]. As shown in Table 4, the water contact angle for PU-H and PU-T coatings is 108° and 115° respectively, which exhibit wettability of coating. Both coatings show a contact angle higher than 90° which shows the hydrophobic nature of the coatings and the results are consistent with the percentage of water absorption. The improvement can be mostly attributed to the extremely hydrophobic nature of long fatty acids chains present in polyesteramide polyol [26]. Furthermore, the PU-T coatings exhibited a high contact angle value compared with PU-H, this difference arises due to the higher crosslink density of PU-T coatings. Due to high crosslink density, the coatings show a hydrophobic nature which prohibits permeation of water droplet and increasing the material's hydrophobicity. Compared to fatty acid based PU coating in the earlier research, a coating with the highest contact angle of 87° [30] and current research the highest contact angle of 115°, that shows that the current coating system is more hydrophobic.

Surface Roughness Properties of PU Coatings

AFM is a widely used technique to examine the surface roughness and three-dimensional (3D) surface topography of coatings. It has been noticed that polyurethanes
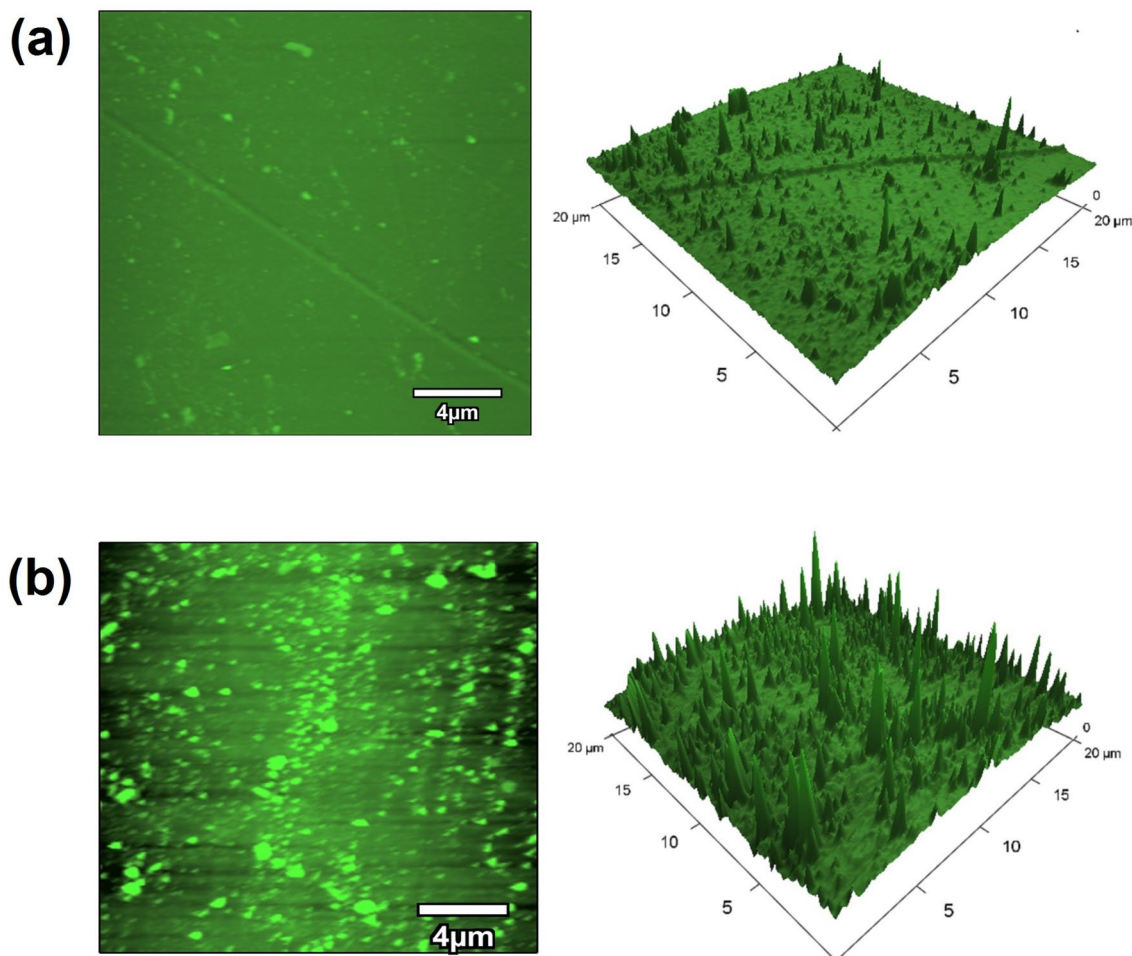
Fig. 12 AFM images of PU coatings. **a** PU-H, **b** PU-T

prepared from various polyol, hardener, and chain extender show the distinctive morphological structure, and numerous factors like surface flexibility and adhesion are all associated with the AFM topographic images [46]. Figure 12 shows the variation in surface topography of both PU coatings. The root mean square of roughness (RMS) was assessed from five randomly selected regions of each coating sample and results presented in Table 4. Topographic images (Fig. 12) and surface roughness values indicate more aggregation of hard segments in PU-T coating which displays a rougher surface than PU-H coating. Increasing hard segments through an aromatic ring of TDI, which is probably the main reason for increasing crosslink density hence the surface roughness of PU-T coating enhances. The surface roughness is influencing the mechanical and hydrophobic properties of coatings, as we can see from Tables 2 and 4, the increase in tensile properties and contact angle values with increases the coating roughness [47].

Conclusion

This study demonstrated that the bio-based sources namely isostearic acid and dimer fatty acids can be exploited for the synthesis of polyesteramide polyol and polyurethane metal coatings. The crosslinking density and rigidity of final PU coatings were modified through structurally different diisocyanates. Moreover, it was also verified that long aliphatic chains from fatty acids contributed to flexibility, hydrophobicity, impact resistance, and elongation properties in final cured PU coatings. After assessing physicomechanical, swelling resistance, surface roughness and coating properties, it was found that PU-T coating exhibited excellent performance due to its higher crosslink density. The PU-coatings showed remarkable results, including a glass transition temperature (T_g) of 53.08−64.18 °C, highest thermal degradation temperature of 352−446 °C, the tensile strength of 10.7−15.5 Mpa, and young modulus of 391.39−452.36 Mpa. Consequently, the PU-T coating showed superior results in comparison to the PU-H coating. This study

encourages the utilization of bio-renewable sources for the synthesis of green polyurethane coatings and offers a sustainable replacement over the conventional petroleum feedstock in the development of coatings.

References

1. Ionescu M, Wan X, Bilic N, Petrovic ZS (2012) Polyols and rigid polyurethane foams from cashew nut shell liquid. J Polym Environ 3:647–658
2. Phalak G, Patil D, Vignesh V, Mhaske S (2018) Development of tri-functional biobased reactive diluent from ricinoleic acid for UV curable coating application. Ind Crop Prod 119:9–21
3. Atabani AE, Silitonga AS, Ong HC, Mahlia TMI, Masjuki HH, Badruddin IA, Fayaz H (2013) Non-edible vegetable oils: a critical evaluation of oil extraction, fatty acid compositions, biodiesel production, characteristics, engine performance and emissions production. Renew Sustain Energy Rev 18:211–245
4. Lu Y, Larock RC (2010) Soybean oil-based, aqueous cationic polyurethane dispersions: synthesis and properties. Prog Org Coatings 69:31–37
5. Ca V, Lligadas G, Ronda JC, Galia M (2013) Renewable polymeric materials from vegetable oils: a perspective. Mater Today 16:337–343
6. Alam M, Akram D, Sharmin E, Zafar F, Ahmad S (2014) Vegetable oil based ecofriendly coating materials: a review article. Arab J Chem 7:469–479
7. Desroches M, Escouvois M, Auvergne R, Caillol S (2013) From vegetable oils to polyurethanes: synthetic routes to polyols and main industrial products. Polym Rev 52:38–79
8. Tan SG, Chow WS (2010) Biobased epoxidized vegetable oils and its greener epoxy blends: a review. Polym Plast Technol Eng 49:1581–1590
9. Kong X, Liu G, Curtis JM (2012) Novel polyurethane produced from canola oil based poly (ether ester) polyols: synthesis, characterization and properties. Eur Polym J 48:2097–2106
10. Ionescu M, Radojcic D, Wan X, Shrestha ML, Petrovic ZS, Upshaw TA (2016) Highly functional polyols from castor oil for rigid polyurethanes. Eur Polym J 84:736–749
11. Fan X, Deng Y, Waterhouse J, Pfromm P (1998) Synthesis and characterization of polyamide resins from soy-based dimer acids and different amides. J Appl Polym Sci 68:305–314
12. Shukla SK, Srivastava K, Srivastava D (2015) Studies on the thermal, mechanical and chemical resistance properties of natural resource derived polymers. Mater Res 18(6):1217–1223
13. Zhang Y, Maxted J, Barber A, Lowe C, Smith R (2013) The durability of clear polyurethane coil coatings studied by FTIR peak fitting. Polym Degrad Stab 98:527–534
14. Chaudhari AB, Tatiya PD, Hedaoo RK, Kulkarni RD, Gite VV (2013) Polyurethane prepared from neem oil polyesteramides for self-healing anticorrosive coatings. Ind Eng Chem Res 52:10189–10197
15. Rajput SD, Mahulikar PP, Gite VV (2014) Biobased dimer fatty acid containing two pack polyurethane for wood finished coatings. Prog Org Coat 77:38–46
16. Kathalewar M, Sabnis A, Melo DD (2014) Polyurethane coatings prepared from CNSL based polyols: synthesis, characterization and properties. Prog Org Coat 77:616–626
17. Parcheta P, Ewa G, Datta J (2020) Effect of bio-based components on the chemical structure, thermal stability and mechanical properties of green thermoplastic polyurethane elastomers. Eur Polym J 123:109422
18. Petrovic ZS, Ferguson J (1992) Polyurethane elastomers. Prog Polym Sci 16:695–836
19. Panda SS, Panda BP, Nayak SK, Mohanty S (2018) A review on waterborne thermosetting polyurethane coatings based on castor oil: synthesis, characterization, and application. Polym Plast Technol Eng 57:500–522
20. Alagi P, Jin Y, Seog J, Chul S (2016) Efficient and quantitative chemical transformation of vegetable oils to polyols through a thiol-ene reaction for thermoplastic polyurethanes. Ind Crop Prod 87:78–88
21. Nelly M, González G, Börjesson P, Levi M, Turri S (2018) Development and life cycle assessment of polyester binders containing 2, 5-furandicarboxylic acid and their polyurethane coatings. J Polym Environ 26:3626–3637
22. Raghunanan LC, Fernandez-prieto S, Martínez I, Valencia C, Sánchez MC, Franco JM (2018) Molecular insights into the mechanisms of humidity-induced changes on the bulk performance of model castor oil derived polyurethane adhesives. Eur Polym J 101:291–303
23. Yang LT, Zhao CS, Dai CL, Fu LY, Lin SQ (2012) Thermal and mechanical properties of polyurethane rigid foam based on epoxidized soybean oil. J Polym Environ 20:230–236
24. Laurichesse S, Huillet C, Avérous L (2014) Original polyols based on organosolv lignin and fatty acids: new bio-based building blocks for segmented polyurethane synthesis. Green Chem 16:3958–3970
25. Liu X, Xu K, Liu H, Cai H, Su J, Fu Z, Guo Y, Chen M (2011) Preparation and properties of waterborne polyurethanes with natural dimer fatty acids based polyester polyol as soft segment. Prog Org Coat 72:612–620
26. Prabhudesai MS, Paraskar PM, Kedar R, Kulkarni RD (2020) Sea buckthorn oil tocopherol extraction's by-product utilization in green synthesis of polyurethane coating. Eur J Lipid Sci Technol 122(4):1–9
27. Petrović ZS, Zhang W, Javni I (2005) Structure and properties of polyurethanes prepared from triglyceride polyols by ozonolysis. Biomacromol 6:713–719
28. Thi T, Hoang K, Kim I (2015) Epoxidation and ring-opening of palm oil to produce high-functionality polyols. Aust J Basic Appl Sci 9(8):89–93
29. Patil CK, Rajput SD, Marathe RJ, Kulkarni RD, Phadnis H, Sohn D, Mahulikar PP, Gite VV (2017) Synthesis of bio-based polyurethane coatings from vegetable oil and dicarboxylic acids. Prog Org Coat 106:87–95
30. Rajput SD, Hundiwale DG, Mahulikar PP, Gite VV (2014) Fatty acids based transparent polyurethane films and coatings. Prog Org Coat 77:1360–1368
31. Ngo HL, Dunn RO, Sharma B, Foglia TA (2011) Synthesis and physical properties of isostearic acids and their esters. Eur J Lipid Sci Technol 113:180–188
32. Ngo HL (2015) Lewis base additives improve the zeolite ferrierite-catalyzed synthesis of isostearic acids. J Am Oil Chem Soc 92:613–619
33. Riazi B, Zhang J, Yee W, Ngo H, Spatari S (2019) Life cycle environmental and cost implications of isostearic acid production for pharmaceutical and personal care products. ACS Sustain Chem Eng 7:15247–15258

34. Zvonkina IJ, Hilt M (2015) Tuning the mechanical performance and adhesion of polyurethane UV cured coatings by composition of acrylic reactive diluents. Prog Org Coat 89:288–296

35. Patil DM, Phalak GA, Mhaske ST (2017) Design and synthesis of bio-based UV curable PU acrylate resin from itaconic acid for coating applications. Des Monomers Polym 20:269–282

36. Chattopadhyay DK, Webster DC (2009) Thermal stability and flame retardancy of polyurethanes. Prog Polym Sci 34:1068–1133

37. Chaudhari A, Gite V, Rajput S, Mahulikar P, Kulkarni R (2013) Development of eco-friendly polyurethane coatings based on neem oil polyetheramide neem oil. Ind Crop Prod 50:550–556

38. Sur S, Choi P, Ko J, Lee J, Lee Y, Kim H (2018) Preparation and properties of DMF-based polyurethanes for wet-type polyurethane artificial leather. Int J Polym Sci 2018:1–9

39. Pathan S, Ahmad S (2013) Synthesis, characterization and the effect of the s-triazine ring on physico-mechanical and electrochemical corrosion resistance performance of waterborne castor oil alkyd. J Mater Chem A 1(45):14227–14238

40. Yadav S, Zafar F, Hasnat A, Ahmad S (2009) Poly (urethane fatty amide) resin from linseed oil—A renewable resource. Prog Org Coat 64:27–32

41. Rajput SD, Gite VV, Mahulikar PP (2014) Renewable source based nonbiodegradable polyurethane coatings from polyesteramide prepared in one-pot using oleic acid. J Am Oil Chem Soc 91:1055–1063

42. Liu X, Zhang R, Zhu J, Jiang Y (2014) Synthesis and properties of full bio-based thermosetting resins from rosin acid and soybean oil: the role of rosin acid derivatives. Green Chem 15:1300–1310

43. Mishra V, Desai J, Patel KI (2018) UV/Oxidative) dual curing polyurethane dispersion from cardanol based polyol: synthesis and characterization. Ind Crop Prod 111:165–178

44. Monteavaro LL, Silva EO, Costa APO, Samios D, Gerbase AE, Petzhold CL (2005) Polyurethane networks from formiated soy polyols: synthesis and mechanical characterization. J Am Oil Chem Soc 82:365–371

45. Liang B, Zhao J, Li G, Huang Y, Yang Z, Yuan T (2019) Facile synthesis and characterization of novel multi-functional bio-based acrylate prepolymers derived from tung oil and its application in UV-curable coatings. Ind Crop Prod 138:111585

46. Wang C, Ma C, Lin W (2017) Tailor-made zwitterionic polyurethane coatings: microstructure, mechanical property and their antimicrobial performance. RSC Adv 7:27522–27529

47. Malkappa K, Jana T (2015) Hydrophobic, water dispersible polyurethane: role of polybutadiene diol structure. Ind Eng Chem Res 54(30):7423–7435